Numerical simulation of gas-liquid two phase flow in micro tubes

Hideo Sunakawa, Susumu Teramoto, Toshio Nagashima
University of Tokyo, Department of Aeronautics and Astronautics
7-3-1 Hongo, Bunkyo-ku, Tokyo 113-8656, JAPAN
hide_s@themo.t.u-tokyo.ac.jp

Keywords: Two-phase Flow, Micro Tube, MARS-VOF

Abstract

Motion of a bubble inside narrow tube is numerically studied. The numerical code assumes axi-symmetric incompressible flow field. The surface of the bubble is captured by VOF (Volume Of Fluid) method, and it is advected by MARS (Multiphase Advection and Reconstruction Scheme). Air bubble inside water is first studied, and it was found that a strong vortex, which is induced by the pressure difference caused by the surface tension, is formed at the rear part of the bubble. Then flow parameters are parametrically varied to understand the correlation between the bubble shape, the bubble velocity, and the flow parameters. The parametric study revealed that the aspect ratio of the bubble mainly depends on *We* number, and the oscillation of the bubble speeds is dependent on *Re* number.

Introduction

Heat exchanger is a device that transports heat from high to low temperature region, and it is indispensable for various applications. Recent development of advanced science and technologies brings high heat generation micro device, therefore more effective compact heat exchanger (CHE) is indispensable. One possible way to enhance heat transfer is to utilize phase change of the coolant in micro tubes and channels. Latent heat and boiling heat transfer make heat exchangers more efficient. However, such heat exchanger has not been put into practice use yet. Technical issues that prevents practical application are

- unsteady boiling phenomena
- scaling effect

In addition to the difficulty in controlling the boiling phenomena, it is also difficult to predict two phase flow in micro tubes with correlations derived from experiences in much larger scale. This is because surface tension and viscosity become dominant in micro tubes, and the flow field would be different from that in normal size. Chen[1] experiments nitrogen-water two phase flow in micro tube (diameter1.0mm and 1.5mm) and observed the flow pattern. Takagi[2] numerically simulated a bubble motion inside micro channel Poiseuille flow, and derived the correlation between pressure loss and the flow field. However, the number of experiment and calculation related to two-phase flow in micro tubes are limited, and two phase flow inside micro passage is not well understood.

In the present study, motion of a bubble inside micro tubes is numerically simulated. The purpose of this study is to discuss how the flow parameters (tube diameter, fluid properties and so on) influence the flow field, and to extend the comprehension about two phase flow in micro tube.

Numerical Scheme

The computation code in this study needs to model transient, incompressible fluid flows with surface tension on free surfaces of general topology. Finite difference solutions to the incompressible Navier-Stokes equations are obtained on an Eulerian rectilinear mesh. The basic algorithm for incompressible flow solution of Navier-Stokes equation is 2 step projection method[3], in which the momentum equation is divided into two steps.

$$\frac{\tilde{\vec{V}} - \vec{V}^n}{\delta t} = -\nabla \cdot (\vec{V}\vec{V})^n + \frac{1}{\rho^n}\nabla \cdot \tau^n + \vec{g}^n + \frac{1}{\rho^n}\vec{F}_b{}^n$$
$$\frac{\vec{V}^{n+1} - \tilde{\vec{V}}}{\delta t} = -\frac{1}{\rho^n}\nabla p^{n+1} \qquad (1)$$

In the first step, intermediate velocity field $\tilde{\vec{V}}$ is calculated from incremental changes resulting from momentum advection, viscosity, gravitational accelerations, and surface tension. The second step requires a solution of a Poisson equation for the pressure field. Momentum advection scheme is van Leer method, which retains second order terms in the Taylor expansion. Momentum advection accuracy reduces to first order (donor cell differencing) near the surface, however. Free surfaces are represented with volume-of-fluid (VOF) data on the mesh. VOF function F is defined as

$$F = \begin{cases} 1 & Liquid \\ 0 & Gas \\ > 0, < 1 & Free\ \ Surface \end{cases} \qquad (2)$$

There are some schemes to capture phase boundary, Front-tracking, Level-set, marker and cell (MAC), etc. VOF scheme has advantage of mass and volume conservation, and ability of representing bubbles coalescence and breakup. However, advection scheme of VOF function needs to conserve fluid volume and

prevent shape dissipation. Donor-Accepter method, which is a classical VOF advection scheme, maintains fluid volume although shapes of bubbles dissipate into square shapes in this method because of the lack of sloped surface transport. Therefore the VOF function advection scheme of the present study is MARS (multi-phase advection and reconstruction scheme)[3]. MARS reconstructs free surfaces considering gradient and advects using fractional step method. This leads to reduction of shape dissipation. Surface tension is modeled as a volume force derived from the continuum surface force (CSF) model[4].

Verification of the Code

A Bubble in Micro Channel

Interaction between bubbles and wall is one of the most important aspects in the analysis of two phase flow in micro path. A rising bubble inside two-dimensional channel is numerically simulated and the results are compared with the results represented by Takagi[2]. The channel width is 0.1mm, and initial flow velocity field is two-dimensional Poiseuille flow which has average velocity of 1m/s. Inlet and outlet conditions are the same. Surface tension coefficient is 1.0dyn/cm, and viscosity is 0.05mg/mm s. Figure 1 is the initial conditions (left) and the calculation results (right) by this code. Pressure loss and bubble shape by the present code is the same as Takagi's result. (Fig.2)

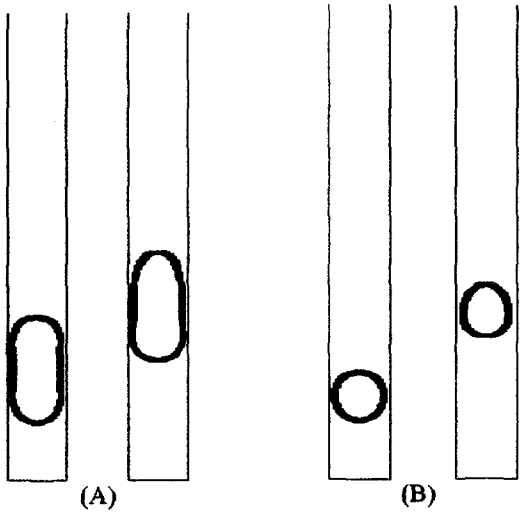

Fig. 1 Bubble shape (T=0, 0.9sec)

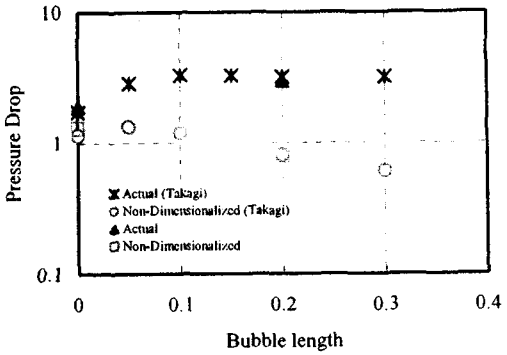

Fig. 2 Pressure drop

Calculation Condition

A bubble motion inside micro circular tube is the object for the calculation. Uniform inlet flow is fed to move the bubble. Working fluids are water and air. Calculation condition is listed on Table1. Reynolds number and Weber number is used on the table. These dimensionless numbers are defined as

$$Re : \frac{\rho UL}{\mu} \qquad We : \frac{\rho LU^2}{\sigma} \tag{3}$$

Initial bubble shapes are shown in figure 3. Front and rear edges of the bubble are sphere shape whose diameter is equal to 80% tube diameter. Length of the straight section is equal to 40% (small) and 80% (large) of tube diameter.

	diameter	inlet velocity	bubble size	*Re*	*We*
Case1	1.0mm	1.0m/s	small	889	13.6
Case2	0.1mm	1.0m/s	small	88.9	1.36
Case2-1	surface tension 1/10 in Case2			88.9	13.6
Case2-2	viscosity 1/10 in Case2			889	1.36
Case2-3	surface tension and viscosity 1/10 in Case2			889	13.6
Case3	0.1mm	$\sqrt{10}$ m/s	small	281	13.6
Case4	0.1mm	$\sqrt{10}$ m/s	large	281	13.6

Table 1 Calculation Pattern

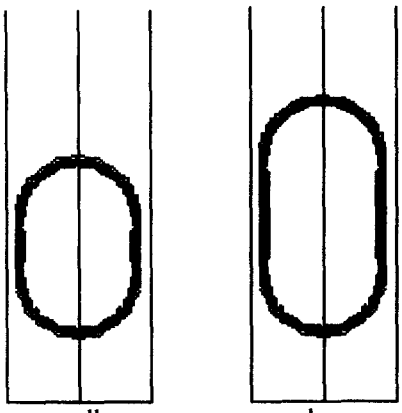

Fig. 3 Initial bubble shape

Results

Flow Field

The flow field around the bubble is characterized by vortices appearing at the rear part of the bubble. Figure 4 shows the velocity vector map around the bubble of Case1. Strong vortex is observed at the rear corner of the bubble, where the curvature of the bubble surface is the maximum. These vortices are caused by the surface tension. According to Laplace equation, surface tension is represented as pressure drop across the gas-liquid interface.

$$\Delta P = \sigma\left(\frac{1}{R_1}+\frac{1}{R_2}\right) \tag{4}$$

The pressure drop is proportional to the surface curvature. The liquid pressure near convex surface becomes lower than the gas region. Pressure is almost constant inside the bubble. Therefore, low pressure region is formed in the liquid near the surface which has strong convex curvature. Figure 5 shows pressure contour (left) and surface tension force contour (right). In figure 5, the low pressure region is observed near the rear corner of the bubble, where the surface tension is the maximum. The curvature of the surface downstream direction of the low pressure region is small, and the pressure drop caused by surface tension is also small. Therefore the pressure at this region becomes higher than the low pressure regions at the corner, and the pressure difference leads to the counter flow from the high pressure region to the low pressure region.

The flow field around the bubble distorts the bubble shape. The characteristic bubble shape is also observed in the experiment by Triplett[6] (Fig.10).

Influence of Fluid Properties Difference

The result of four cases, Case2, Case2-1 (surface tension 1/10 of Case2), Case2-2 (viscosity 1/10 of Case2) and Case2-3 (surface tension and viscosity 1/10 of Case2) are compared, and correlation between flow properties, bubble shape and bubble velocity is discussed.

1. Bubble Shape

In Case2 (Fig.7), the bubble shape is nearly round shape. Velocity vector map around the bubble and pressure contour of Case2-1 is shown in Fig.8. Surface tension in Case2-1 is 1/10 of Case2, therefore the surface tension force which makes the bubble round is weaker and the bubble shape becomes vertically long. In Case2-2 (Fig.9), in which the viscosity is 1/10 of Case2, surface tension becomes relatively strong because of low viscosity, and this leads to bubble shape much closer to circle than in Case2. In Case2-3 (Fig.10), the rear part of the bubble is enlarged compared to that in Case2-1 (surface tension 1/10).

The variation of the bubble shape is discussed more clearly based on dimensionless numbers (Reynolds number and Weber number). Weber number on the bubble shape is considered by comparing Case2 (small *We*) and Case2-1 (large *We*), and Case2-2 (small *We*) and Case2-3 (large *We*). The bubble shape of small Weber number differs substantially from that of large Weber number. Small Weber number (about *We*=1.36) leads to round bubble shape, though large Weber number (about *We*=13.6) brings bullet-like shape. They show that Weber number has large influence on the bubble shape.

To discuss the results with different Reynolds number. Case2 (large *Re*) is compared with Case2-2 (large *Re*). The bubble shape in Case2-2 is closer to circle than in Case2, however, the difference caused by Reynolds number is smaller than that caused by Weber number. Comparison between Case2-1 (small *Re*) and Case2-3 (large *Re*) show that although the bubble in Case2-3 shows the expansion at the rear, it is not major difference compared to the difference caused by Weber number. Hence Reynolds number does not influence bubble shape compared to Weber number.

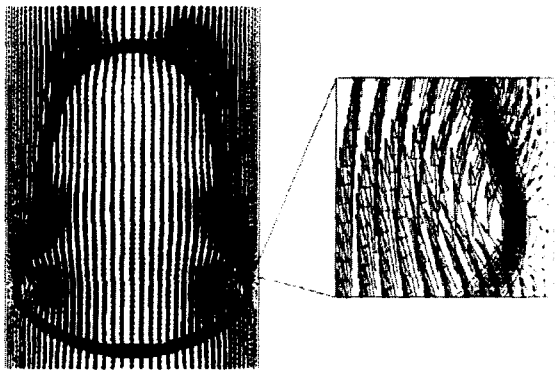

Fig. 4 Bubble shape with flow field (Case1)

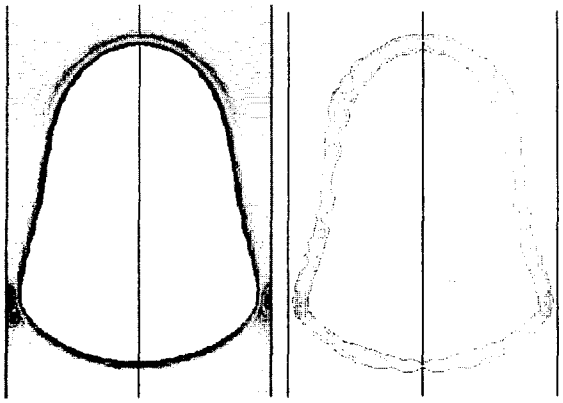

Fig. 5 Pressure contour and surface tension force (Case1)

Fig. 6 Experiment by K.A.Triplett[6]

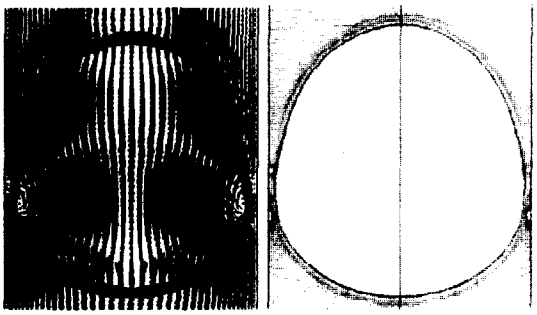

Fig. 7 Bubble shape with flow field and pressure contour (Case2)

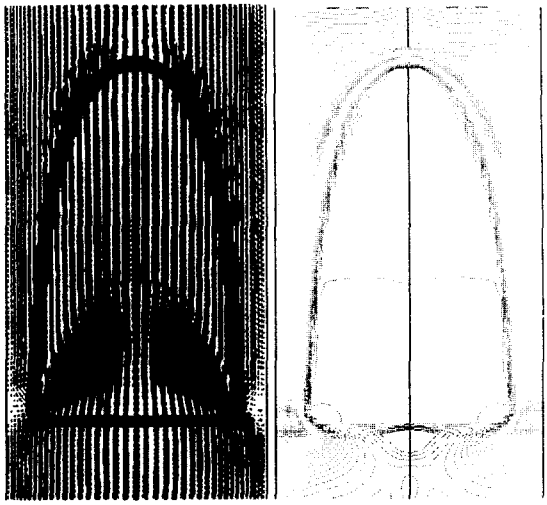

Fig. 8 Bubble shape with flow field and pressure contour (Case2-1)

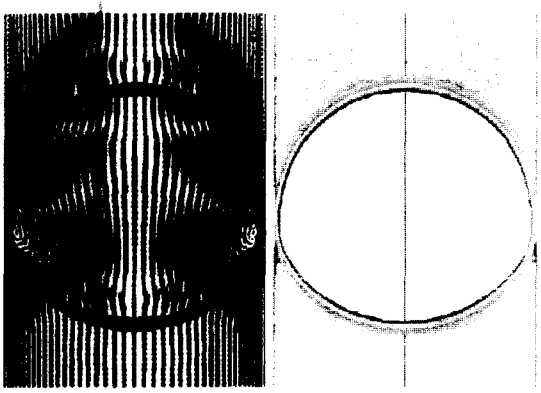

Fig. 9 Bubble shape with flow field and pressure contour (Case2-2)

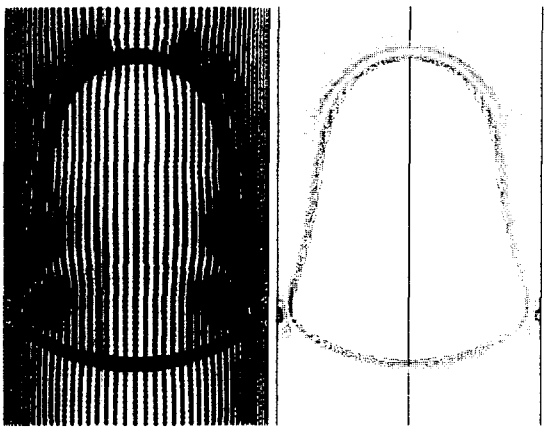

Fig. 10 Bubble shape with flow field and pressure contour (Case2-3)

2. Bubble Velocity

Bubble velocities are plotted in figure 11. The bubble velocity reaches steady speed in Case2 and Case2-1 while the bubble velocity shows oscillation in Case2-2 and Case2-3. This is the viscosity effect. Former two cases have low Reynolds number (about Re=88.9), and latter two cases have high Reynolds number (about Re=889). Strong viscosity prevents the bubble from oscillating. Hence Reynolds number is the important factor of the bubble oscillation.

From the viewpoint of average bubble speed, Case1-1 (1.49m/s) is the fastest, Case2-3 (1.17m/s) is the second place, then Case2 (1.10m/s), and Case2-2 (0.98m/s) is the slowest. The order of the bubble speed coincides with the order of the thickness of the liquid layer between the bubble and the wall. Thicker the liquid layer is, faster the bubble velocity becomes.

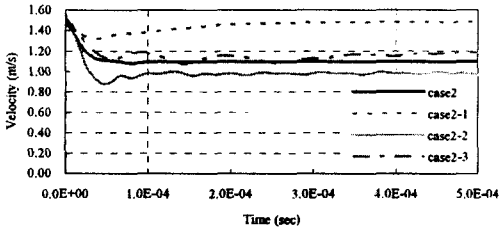

Fig. 11 Velocity (Case2, Case2-1, Case2-2,Case2-3)

Influence of by Inlet Velocity

The inlet velocity in Case3 is $\sqrt{10}$ m/s so that the Weber number is equal to that in Case2-3. The velocity vector map around the bubble and the pressure contour is shown in figure 12. The bubble shape of Case3 is identical to that of Case2-3. These observations support that Weber number is the primary factor in determining the bubble shape.

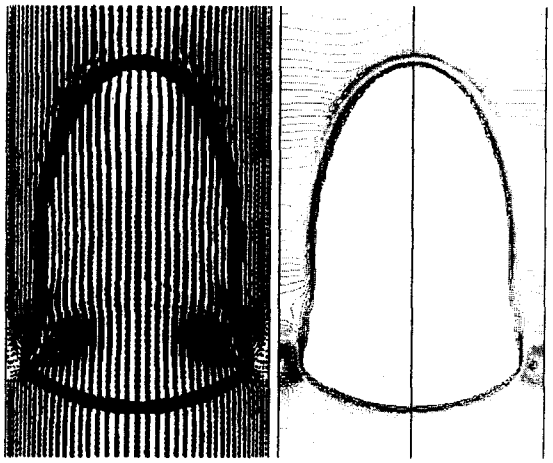

Fig. 12 Bubble shape with flow field and pressure contour (Case3)

Influence of Initial Bubble Shape

To capture the influence of the initial bubble shape, Case3 (small initial bubble) and Case4 (large initial bubble) are compared.

Because the bubble in Case4 (Fig.13) is larger than in Case3, the bubble in Case4 is longer and the liquid layer between the bubble and the wall is thinner than in Case3. Velocity plot is shown in figure 14. The bubble velocity in Case 4 (3.05m/s) is slower than in Case3 (3.13m/s). Because of the thin liquid layer, the bubble velocity in Case4 is less than in Case3.

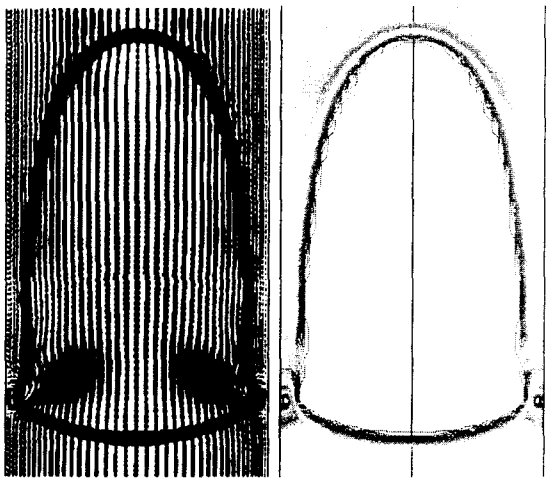

Fig. 13 Bubble shape with flow field and pressure contour (Case4)

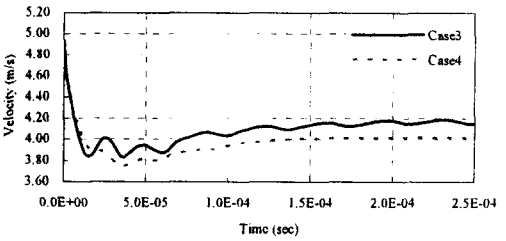

Fig. 14 Velocity (Case3, Case4)

Conclusion

The numerical analysis of a bubble motion in micro tube is carried out, and the correlation between the parameters (diameter, fluid properties, inlet velocity, and initial bubble shape) and the bubble shape and velocity is discussed.

In all cases, surface tension causes the vortex behind the bubble, and it distorts the bubble shape.

Reynolds number is associated with bubble oscillation, and Weber number is connected with bubble shape. Bubble velocity is dependent on the thickness of the

liquid layer between the bubble and the wall. Thicker the liquid layer is, faster the bubble velocity becomes.

References

1) W.L.Chen , M.C.Twu and C.Pan : Gas- liquid two-phase flow in micro-channels, International Journal of Multiphase Flow 28, 2002 pp.1235-1247
2) Shu Takagi, Kazuyasu Sugiyama, Osamu Nakabepu, Yoichiro Matsumoto, : Numerical Analysis of a Deformed Bubble in Micr-Channel, 1998-7 in Japan
3) D.B.Kothe and R.C.Mjolsness : RIPPLE: A New Model for Incompressible Flows with Free Surfaces, AIAA Journal Vol.30, No.11, November, 1992
4) Tomoaki Kunugi : MARS for Multiphase Calculation, February 10, 2000
5) J.U.Brackbill , D.B.Kothe and C. Zemach :A continuum Method for Modeling Surface Tension, Journal of Compu- tational Physics 100, 1992 pp. 335-354
6) K.A. Triplett, S.M. Ghiaasiaan, S.I. Abdel-Khalik, D.L. Sadowski : Gas-liquid two-phase flow in microchannels Part I: two-phase flow patterns, International Journal of Multiphase Flow 25, 1999 pp. 377-394